

Role of mesenchymal stem cells and taurine in chronic pancreatitis in adult albino rats

Nahla S. Saad, Ghada S. El-dien Abdelkader, Noha A.H. Salem, Mona H. Mohammed Ali, Magdy M.O. El-Fark

Human Anatomy and Embryology Department, Faculty of Medicine, Suez Canal University, Ismailia, Egypt

SUMMARY

Chronic pancreatitis (CP) is an inflammatory disease of the pancreas that leads to pancreatic fibrosis. The current treatment of the disease is not efficient or adequate. Therefore, more efficient interventions are required to diminish the substantial burden of the disease.

The present study aimed to assess the potential therapeutic value of bone marrow-derived mesenchymal stem cells (BMSCs) and/or taurine supplementation in CP-induced, using intraperitoneal injection of L-arginine. Forty-five rats were randomly divided into five groups (9 rats each): 1) control group, 2) CP group, 3) CP+BMSCs, 4) CP+Taurine, and 5) CP+BMSCs+Taurine. At the end of the experimental period, the pancreatic tissues were collected, weighed, and prepared for light, electron, and immunohistochemical (α -SMA) microscopic examination. The CP group showed destruction of the pancreatic tissues including fatty degeneration, minimal zymogen granules, and focal degranulation of the rER. Some of the islets degenerated with intense immunoreactivity of α -SMA in the stroma. The groups treated with BMSCs or taurine alone showed improvement of the pancreatic architecture with the presence of some cytoplasmic vacuolation, fewer zymogen granules than the control group, and minimal in-

flammatory cell infiltrate. The CP+BMSCs+Taurine group showed apparently normal architecture. The combined therapy of both BMSCs and taurine could ameliorate CP progression by suppressing inflammation and fibrosis.

Key words: Chronic pancreatitis – Mesenchymal stem cells – Taurine – L-arginine

INTRODUCTION

Chronic pancreatitis (CP) is a pathological fibro-inflammatory syndrome of the pancreas in individuals with genetic, environmental, and/or other contributing risk factors that develop persistent pathological responses to parenchymal injury or stress. CP results in the development of diabetes mellitus and/or maldigestion due to endocrine and exocrine insufficiency. Moreover, CP patients have an increased risk of developing pancreatic adenocarcinoma with increased overall mortality (Whitcomb et al., 2016).

The pathophysiology of CP is complex and not completely understood (JC and Parks, 2021). Additionally, the current treatments for CP mainly target the symptoms rather than the pathological process (Singh et al., 2019).

Corresponding author:

Magdy M. Omar El-Fark. Human Anatomy and Embryology Department, Faculty of Medicine, Suez Canal University, 4.5 Km the Ring Road, Ismailia, Egypt. Phone: +201228282092. E-mail: magdy_omar@med.suez.edu.eg / anatomist1996@yahoo.com

Submitted: January 30, 2023. Accepted: March 28, 2023

<https://doi.org/10.52083/JKLG9096>

Mesenchymal stem cells (MSCs) are a subset of the mesodermal adult stem cells population that is present in numerous living tissues including bone marrow, adipose tissue, and amniotic fluid. As a result of MSCs' immunomodulatory capabilities, and differentiation potential to any type of cells, they have a driving force of regenerative medicine (Andrzejewska et al., 2019). However, only a few studies have explored the therapeutic potential of MSCs on CP (Scuteri and Monfrini, 2018).

Taurine, 2-aminoethanesulfonic acid, is a semi-essential amino acid, which acts as an anti-inflammatory and antioxidant, and is protective against lipid peroxidation, reperfusion injury, and excessive extracellular matrix deposition. It has been demonstrated that the administration of taurine could improve pancreatic fibrosis in an experimental model of CP (Shirahige et al., 2008).

This study was conducted to evaluate the possible therapeutic role of BMSCs and taurine supplementation, alone or in combination, for the treatment of CP in L-arginine-injection-induced chronic pancreatitis.

MATERIALS AND METHODS

Animals

Fifty-one (forty-five females and six males) adult albino rats were used, with an average weight of ≥ 250 g. Animals were kept in the animal house of the Faculty of Medicine, Suez Canal University. All animals were housed in special wire mesh cages at room temperature with regular day and night cycles with water and food ad libitum. Rats were kept for 2 weeks before the start of the experiment for acclimatization. Male rats were used only as a source for MSCs (Marrache et al., 2008). The Research Ethics Committee of the Faculty of Medicine, Suez Canal University, Egypt, examined and approved this study protocol (SCU3253). The study followed the National Institutes of Health's guidelines for the handling and use of laboratory animals (NIH Publications No. 85-23, revised 1996).

Chemicals

L-arginine monohydrochloride: Powder (L-arginine – reagent grade, $\geq 98\%$), obtained from Sigma Chemical St. Louis, MO, USA.

Taurine extra pure: Molecular weight 125.15, obtained from Alpha Chemika (400 053, Maharashtra, India).

BMSCs isolation and culture

This was carried out at the Center of Excellence in Molecular and Cellular Medicine, Suez Canal University. BMSCs were obtained from the femora and tibiae of the male rats after scarification and extraction in complete aseptic conditions. Cells were cultured in complete media (DMEM + 10% FCS + 1% Penicillin/streptomycin) and incubated at 37°C humidified atmosphere containing a 5% CO₂ (Lotfy et al., 2014). Media were changed every 3 days until the cells reached 90-100% of confluence on the twelfth day, and then the cells were harvested through trypsinization to be subcultured for 3 days. BMSCs were harvested and cell mixtures of 2×10^6 /ml of PBL were prepared (Huang et al., 2015).

Flow cytometry analysis

This was carried out at NSA Lab Cairo, Egypt. Approximately 1×10^6 BMSCs at the second passage were harvested. Cell preparations were treated with the monoclonal antibody against CD34 labeled with fluorescein isothiocyanate (FITC), and against CD44 labeled with phycoerythrin (PE). The protocols used were those described by the manufacturer. The cell preparations were analyzed by the flow cytometer (Calibur, BD, USA) for the expression of the mentioned markers (Li et al., 2014).

PCR detection of male-derived BMSCs

This was carried out at the Applied Biotechnology Lab, Ismailia, Egypt. Primer sequences for *SRY* gene (forward 5'-AGATCTTGATTTTGTAGTGTTC-3'), (reverse 5'-TGCAGCTCTACTC-CAGTCTTG-3') were obtained and mixed with 1 μ g pancreatic DNA and Taq polymerase. The PCR products were separated by electrophoresis in 0.8% agarose gel and stained with ethidium bromide. Agarose gel of PCR products of *SRY* gene was detected as a Trans-illuminated line (An et al., 1997).

Experimental Design

Forty-five female rats were randomly divided into five groups (9 rats each) as the following:

- Group A: control (sham) group: rats received two IP injections of normal saline 1 hour apart on day 1, followed by additional injections on days four, seven, and ten in the same way as day 1 (González et al., 2011).
- Group B: chronic pancreatitis-induced group (CP): rats were kept fasted for 12 hours, then received two injections of 20% L-arginine hydrochloride in normal saline solution at a dose of 200 mg/100 g body 1 hour apart on day 1 (Soliman et al., 2014), followed by injections on days four, seven and ten in the same manner as day 1 (González et al., 2011).
- Group C: chronic pancreatitis treated with bone marrow mesenchymal stem cells group (CP+BMSCs): chronic pancreatitis was induced as in group B. On the 5th day after the last L-arginine injection, rats were injected once with 2×10^6 BMSCs, intravenous (IV) through the tail vein in 100 μ L of phosphate buffered solution (PBS) per animal (Zhou et al., 2013).
- Group D: chronic pancreatitis treated with taurine group (CP+Taurine). Chronic pancreatitis was induced as in group B. On the 5th day after the last L-arginine injection, rats were treated with IP taurine injection once daily at a dose of 1000 mg/kg for four weeks (Mas et al., 2006).
- Group E: chronic pancreatitis treated with BMSCs and taurine group (CP+BMSCs+Taurine). Chronic pancreatitis was induced as in group B. On the 5th day after the last L-arginine injection, rats were treated with both BMSCs and taurine in the same dose and course as previously mentioned (Yusop et al., 2018).

All rats were sacrificed at the end of the experiment by cervical decapitation. The pancreas was extracted, weighed, and divided into two parts; one was prepared for light microscopy and the second for electron microscopy.

Light microscopic examination of the pancreas

The prepared pancreatic tissues were stained with haematoxylin and eosin (H&E) stain. Slides

were examined by Olympus DP70 light microscope (Tokyo, Japan).

Immunohistochemical staining

Endogenous peroxidase of deparaffinized sections was blocked with 3% hydrogen peroxide. Sections were incubated overnight at 4°C with a monoclonal antibody mouse α -SMA (1:800 dilutions, Santa Cruz, California, USA). Envision™ Detection Kit was used for antibody detection (Yang et al., 2012).

Transmission electron microscopic (TEM) examination

Pancreatic specimens were fixed in 2% buffered glutaraldehyde, washed then dehydrated in alcohol, and embedded in epoxy resins. Semithin sections were cut at 1 μ m thickness followed by Ultrathin sections (80-90 nm) obtained and stained with uranyl acetate and lead citrate (Bozzola and Russell, 1999). The sections were examined with a JEOL-1010 (Japan) transmission electron microscope (TEM), at the regional center for Mycology and Biotechnology transmitting electron unit (Al-Azhar University, Cairo, Egypt), and photographed under different magnifications.

Morphometric study

In α -SMA immunostained sections, the surface area percentage of immunostained sections were measured in five non-overlapping fields from five different sections at a magnification of 100/slide using ImageJ 2 software.

Statistical analysis

Data processing and analysis were done through SPSS V.24. ANOVA test with Bonferroni post-hoc test. Data were expressed as mean and standard deviation. Significance was considered when P-value was less than 0.05 ($P < 0.05$).

RESULTS

Cultivation and characterization of rat BMSCs

Bone marrow cells were incubated at 37°C with 5% CO₂. On day 1, the cells were floating, rounded, and small with a central nucleus (Fig. 1A). On the

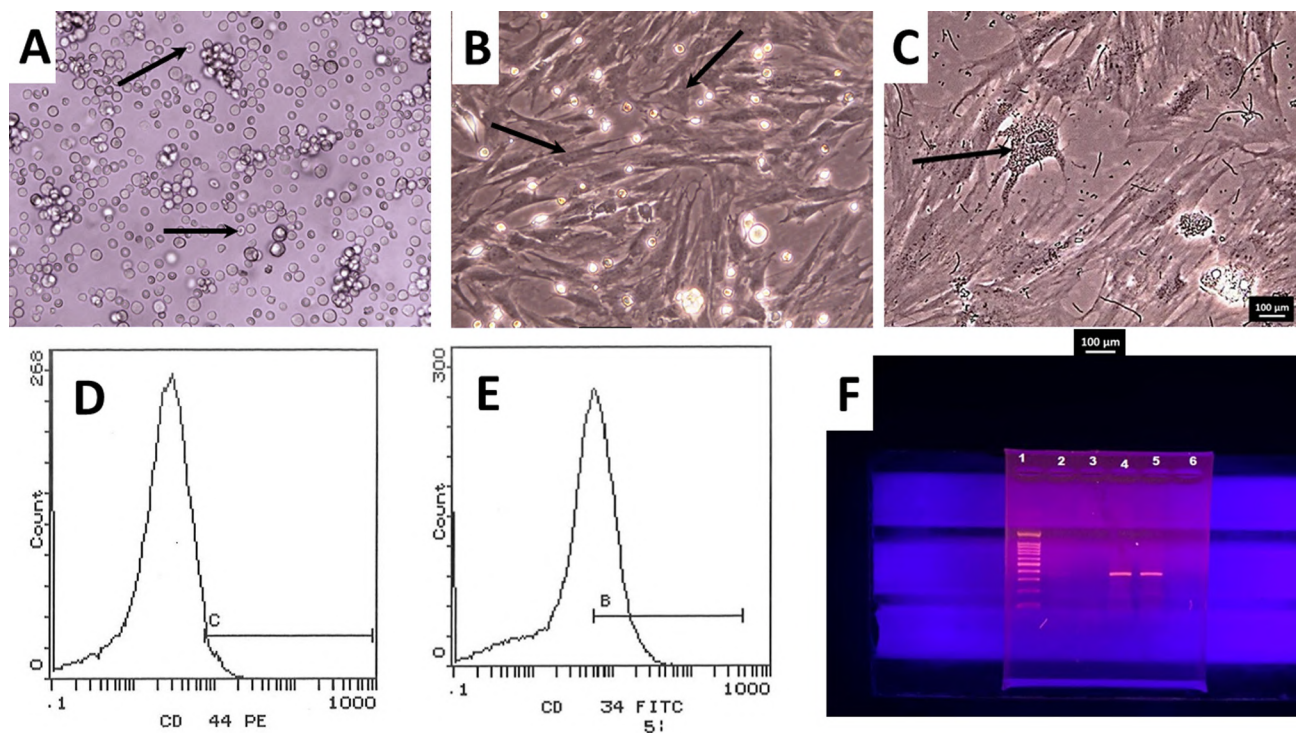


Fig. 1.- Photomicrographs of the cultured BMSCs. **(A)** On the 1st day of incubation; they appeared rounded, floating with a central nucleus (arrows). **(B)** On the 8th day of incubation; spindle-shaped BMSCs were formed (arrows) that reached about 80% confluence. **(C)** On the 3rd day of subculture; the cells had a polygonal appearance, prominent nucleolus, and cell processes (arrow). Scale bar = 100 μ m. **(D)** Flow cytometry analysis of BMSCs showing positive expression of CD 44 and **(E)** negative expression of BMSCs of CD 34. **(F)** PCR product was obtained from the reaction of the primer with pancreatic genomic DNA. The first lane was the standards /100 base pair ladder; the second, third, and sixth lanes are empty which were of groups A, B, and D. Fourth and fifth lanes are positive for *SRY* gene which were of groups C and E. BMSCs, bone marrow mesenchymal stem cells; PCR, polymerase chain reaction.

8th day of incubation, adherent spindle-shaped BMSCs were formed with about 80% confluence (Fig. 1B). On the 12th day, a cell sheet of BMSCs was formed that reached about 100% confluence. Cells were harvested and subcultured at 37°C with 5% CO₂. On the 3rd day of the subculture, well-defined BMSCs were seen having a polygonal appearance with a prominent nucleolus and a well-defined cell process (Fig. 1C).

Flow cytometric analysis of BMSCs surface markers of the subcultured cells revealed moderate positive expression of CD 44 marker in most of the adherent cells (43%) (Fig. 1D).

On the other hand, the majority of adherent cells were negative for CD 34 surface marker expression, with only 4% of the cells being positive (Fig. 1E).

The male *SRY* gene was successfully traced in the rat pancreas of groups C and E, which were treated by BMSCs. In contrast, the test failed to trace the male *SRY* sequences in the pancreatic tissue of the other groups (Fig. 1F).

Body weight assessment (Table 1)

The initial body weights were approximated among the study groups. Rats in two groups showed weight gain (Control and CP+BMSCs+Tau-

Table1. Weight parameters (g) in different study groups.

	Control	CP	CP+BMSCs	CP+Taurine	CP+BMSCs + Taurine
Initial body weight	263.6±2.8	264.3±9.2	262.7±9.2	260.1±6.5	262.0±6.9
Final body weight	278.0± 5.0	244.6± 11.1	258.0± 8.5	253.2± 10.0	271.0± 10.1
Body weight (gain/loss)	18.4±3.8	-19.8±3.5 ^{b,c,d,f}	-3.7±8.8 ^{b,e}	-6.9±4.9 ^{b,f}	7.0±4.3 ^a
Weight of the pancreas	3.06± 0.18	2.08± 0.28 ^{b,f}	2.49± 0.26 ^a	2.21± 0.36 ^{b,e}	2.77± 0.37

Results are expressed as Mean ± SD, n= (9). Significance of differences among groups was evaluated by one-way ANOVA followed by Bonferroni Post Hoc Test.

a- P<0.01 vs. control group. **b-** P<0.001 vs. control group. **c-** P <0.001 vs. CP+BMSCs group. **d-** P<0.001 vs. CP+Taurine group. **e-** P<0.01 vs. CP+BMSCs+Taurine group. **f-** P <0.001 vs. CP+BMSCs+Taurine group.

rine). This increase in the body weight at the end of the study was in the control group 18.4 ± 3.8 , representing an increase of 6.98% from the initial body weight; and, in the CP+BMSCs+Taurine group, 7.0 ± 4.3 , representing an increase by 2.67% from the initial body weight. Rats in the other three treated groups showed weight loss (CP, CP+BMSCs, and CP+Taurine). This decrease in the body weight at the end of the study recorded in the CP group was -19.8 ± 3.5 , representing a decrease of 7.49% from the initial body weight; in the CP+BMSCs group, -3.7 ± 8.8 , representing a decrease by 1.41% from the initial body weight; and in the CP+Taurine group, -6.9 ± 4.9 , representing a decrease by 2.65% from the initial body weight. When compared to the control group, there was a significant decrease in body weight in different study groups; CP ($P < 0.001$), CP+BMSCs ($P < 0.001$), CP+Taurine ($P < 0.001$), and CP+BMSCs+Taurine ($P < 0.01$). There was a significant decrease ($P < 0.001$) in body weight at the end of the study in rats in the CP group when compared to the CP+BMSCs, CP+Taurine, and CP+BMSCs+Taurine groups. In the three groups treated with BMSCs and taurine, the CP+BMSCs+Taurine group showed a considerable increase in weight gain; there was a significant decrease in body weight at the end of the study in both the CP+BMSCs ($P < 0.01$) and CP+Taurine ($P < 0.001$) groups, when compared to the CP+BMSCs+Taurine group.

Weight of the pancreas (Table 1)

Rats in the control group showed a pancreatic weight of 3.06 ± 0.18 g. There was a decrease in the weight of the pancreas with different degrees in the four treated groups, with the lowest values in the CP (2.08 ± 0.28), CP+Taurine (2.21 ± 0.36), and CP+BMSCs (2.49 ± 0.26) groups, and the highest value among these four treated groups was in the CP+BMSCs+Taurine group (2.77 ± 0.37). The decrease in the weight of the pancreas was significant in both the CP and CP+Taurine groups ($P < 0.001$), and CP+BMSCs ($P < 0.01$) when compared to the control group. Rats in the CP+BMSCs+Taurine group showed a non-significant decrease in the weight of the pancreas when compared to the control group. On the other hand, there was a significant decrease in the

weight of the pancreas in both the CP ($P < 0.001$) and CP+Taurine groups ($P < 0.00$) when compared to the CP+BMSCs+Taurine group.

Light microscopic examination of the pancreas

H&E-stained sections of the pancreas of the control group showed pancreatic lobules of closely packed acini forming the main bulk of the gland and islets of Langerhans. The pancreatic acini were seen formed of wedge-shaped cells arranged around a central narrow lumen. The cells were with basophilic cytoplasm, basal rounded vesicular nuclei with prominent nucleoli, and apical acidophilic secretory zymogen granules. The centro-acinar cells appeared at the central lumen of the acini representing the beginning of the duct system of the exocrine pancreas, the lobules were separated by interlobular septae containing blood vessels and interlobular ducts with cuboidal epithelium, filled with homogeneous colloid material, and surrounded by connective tissue (Fig. 2A).

The islets of Langerhans varied in size and were composed of masses and cords of secretory cells with numerous fenestrated capillaries in-between. Some endocrine cells exhibited pale acidophilic cytoplasm and pale prominent nuclei mostly situated at the center. Other cells with strong acidophilic cytoplasm and dark nuclei were found mainly at the periphery of the islets. The blood capillaries within the islets were recognized by the flat nuclei of the capillary endothelium. (Fig. 2B). Sections of the CP group showed severe destruction of the acinar cells' architecture, with areas of fatty degeneration. There were multiple dilated congested blood vessels and inflammatory cells infiltrate (Fig. 2C). The interlobular duct showed glandular hyperplasia in the form of an increased number and size of the pancreatic ductal glands. Some of the islets of Langerhans degenerated with dark pyknotic nuclei. (Fig. 2D). Sections of the CP+BMSCs group showed less pancreatic destruction. Some acini showed cytoplasmic vacuolation with a reduction of their zymogen granules accompanied by minimal inflammatory cell infiltrate (Fig. 3A). Moreover, congestion of blood vessels was still evident and a few areas of the islet of Langerhans' cellular degeneration were still present (Fig. 3B). In CP+Taurine, taurine administra-

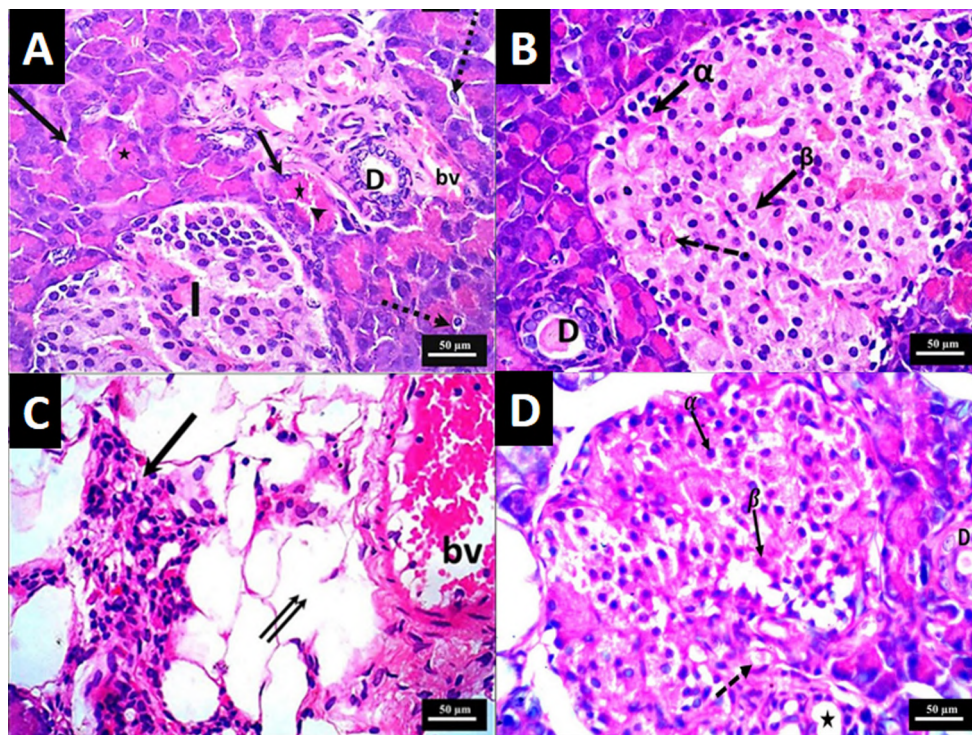


Fig. 2.- H&E-stained sections of the pancreas. **(A)** The control group had the pancreatic acini formed of wedge-shaped cells arranged around a central narrow lumen (arrowhead). The cells had basal rounded vesicular nuclei (arrow), apical acidophilic granules (*), centroacinar cells (dashed arrow), an islet of Langerhans (I), blood vessel (bv), and intralobular duct (D). **(B)** A pale stained islet of Langerhans of the control group that was rich in capillaries (dashed arrow). Some endocrine cells have pale acidophilic cytoplasm and pale prominent nuclei (β), while other cells have strongly acidophilic cytoplasm and dark nuclei (α) and intralobular duct filled with the colloid material (D). **(C)** The CP group showed massive acinar destruction (double arrow), and inflammatory cell infiltrates (arrow), with congested and dilated blood vessels (bv). **(D)** The islets of Langerhans of the CP group showed dilated blood capillaries (dashed arrow), areas of degeneration (*), cells with a pale nucleus and pale cytoplasm (β), cells with a dark nucleus and acidophilic cytoplasm (α). H&E, x400; scale bars = 50 μ m. H&E, hematoxylin and eosin; CP, chronic pancreatitis.

tion reduced the pancreatic tissue destruction induced by L-arginine, despite the presence of areas of tissue degeneration in the form of vacuolation of the cytoplasm and fatty infiltration. However, these changes were less than that noticed in the CP group (Fig. 3C). The islets of Langerhans showed small areas of cellular degeneration with some apoptotic bodies and vascular congestion (Fig. 3D). The pancreas of the CP+BMSCs+Taurine group showed nearly normal architecture similar to that of the control group with the restoration of the secretory acini with their basal basophilia and apical acidophilia of the zymogen granules. Few vacuolations were seen within some acini.

Normal interlobular ducts and blood vessels were noticed in the interlobular spaces (Fig. 3E). The islets of Langerhans showed apparent normal structure, like that of the control group, with cells of pale nuclei and cytoplasm at the center and cells with strong acidophilic cytoplasm and dark nuclei found mainly at the periphery of the islets (Fig. 3F).

Alpha smooth muscle actin (α -SMA) immunohistochemistry

The pancreas of the control group showed minimal expression of α -SMA in the smooth muscle cells in the wall of the blood vessels, with negative expression in the wall of the ducts, stroma, and islet of Langerhans. (Fig. 4A). The CP group showed intense immunoreactivity of α -SMA in the stroma, also around the ducts and blood vessels, with minimal expression in the islets of Langerhans (Fig. 4B). The CP+BMSCs group showed moderate expression of α -SMA immunoreactivity in the stroma around the blood vessels and ducts, with negative expression in the islet of Langerhans (Fig. 4C). The CP+Taurine treated group showed moderate immunoreactivity of α -SMA in the stroma around the blood vessels and ducts, with minimal expression in the islets of Langerhans (Fig. 4D).

The CP+BMSCs+Taurine group showed minimal immunoreactivity of α -SMA around the stromal

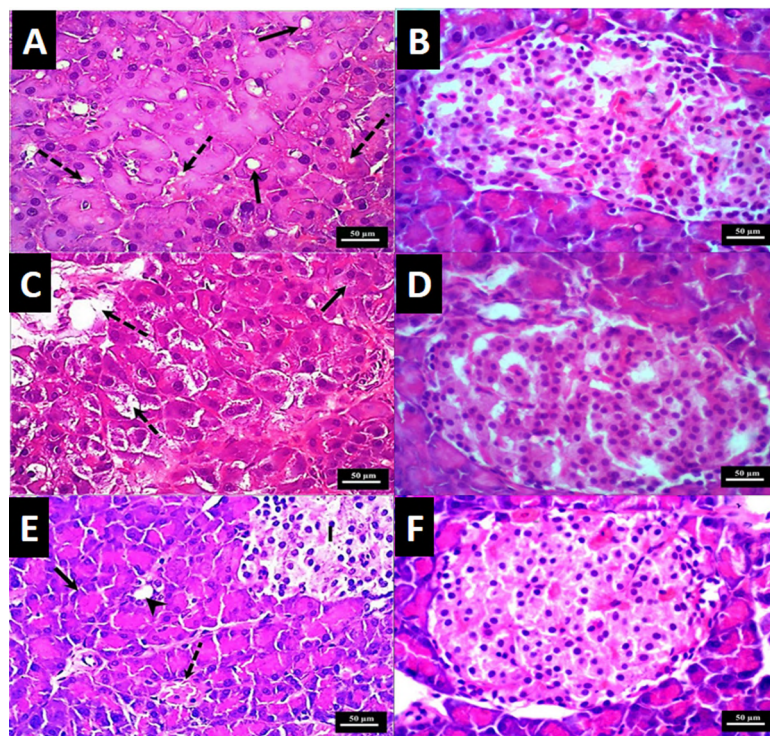


Fig. 3.- H&E-stained sections of the pancreas. **(A)** CP+BMSCs group showing preservation of most of the acinar architecture. Some acini show vacuolation of their cytoplasm (dashed arrows) with decreased zymogen granules and fatty infiltration (arrows). **(B)** CP+BMSCs group showing islets of Langerhans, with small areas of tissue degeneration in between their cords of cells. **(C)** CP+Taurine group showing areas of tissue degeneration (dashed arrows) intermingled with normal acinar architecture (arrow). **(D)** CP+Taurine group showing an islet of Langerhans with nearly normal architecture with few areas of cellular degeneration. **(E)** the CP+BMSCs+Taurine group showed pancreatic acini with nearly normal architecture (arrow), intralobular duct (arrowhead), normal blood vessel (dashed arrow), and the islet of Langerhans (I). **(F)** CP+BMSCs+Taurine group shows islet of Langerhans with a structure resembling that of the control group. H&E, x400; scale bars = 50 µm. H&E, hematoxylin and eosin; CP, chronic pancreatitis; BMSCs, bone marrow mesenchymal stem cells.

blood vessels and ducts, with negative expression in the islet of Langerhans (Fig. 4E).

Area percentage of α -SMA immunostaining

The pancreas of the control group showed a minimal value of area percentage of α -SMA immunostaining (1.89 ± 0.62); rats in the CP group showed a high area percentage of α -SMA immunostaining (30.22 ± 4.78), while the other three treated groups showed lower percentages of α -SMA immunostaining as follows: CP+BMSCs, 8.8 ± 4.06 ; CP+Taurine, 8.16 ± 4.17 , and, finally, CP+BMSCs+Taurine, 4.37 ± 0.86). There was a significant increase in the area percentage of α -SMA immunostaining in the CP group when compared to the control ($P < 0.01$), CP+Taurine ($P < 0.05$), CP+BMSCs ($P < 0.05$), and CP+BMSCs+Taurine ($P < 0.05$) groups. On the other hand, the CP groups treated with BMSCs alone, taurine alone, or with a combination of both showed a non-significant increase in the area percentage of α -SMA immunostaining when compared to the control group. (Fig. 5).

Transmission electron microscopy (TEM)

Ultrathin examination of the pancreatic acini of the control group showed pyramidal acinar cells and intercellular space containing interdigitations of adjacent cells, representing canaliculi that are connected to the acinar lumen. The acinar cells appeared to have basally located, spherical, euchromatic nuclei with prominent nucleoli. Variable-sized electron-dense secretory zymogen granules occupied most of the apical portion of the cytoplasmic compartment. The rough endoplasmic reticulum lay adjacent to the nucleus and was heavily studded with ribosomes. The mitochondria were scattered in-between the rough endoplasmic reticulum and contained fairly arranged parallel shelf-like cisternae (Fig. 6A). The ultrastructure of β cell of islets of Langerhans showed euchromatic nuclei with prominent nucleoli and evenly distributed chromatin with some concentration at the nuclear membrane, abundant secretory granules of varying sizes with electron-lucent halo structure between the limiting

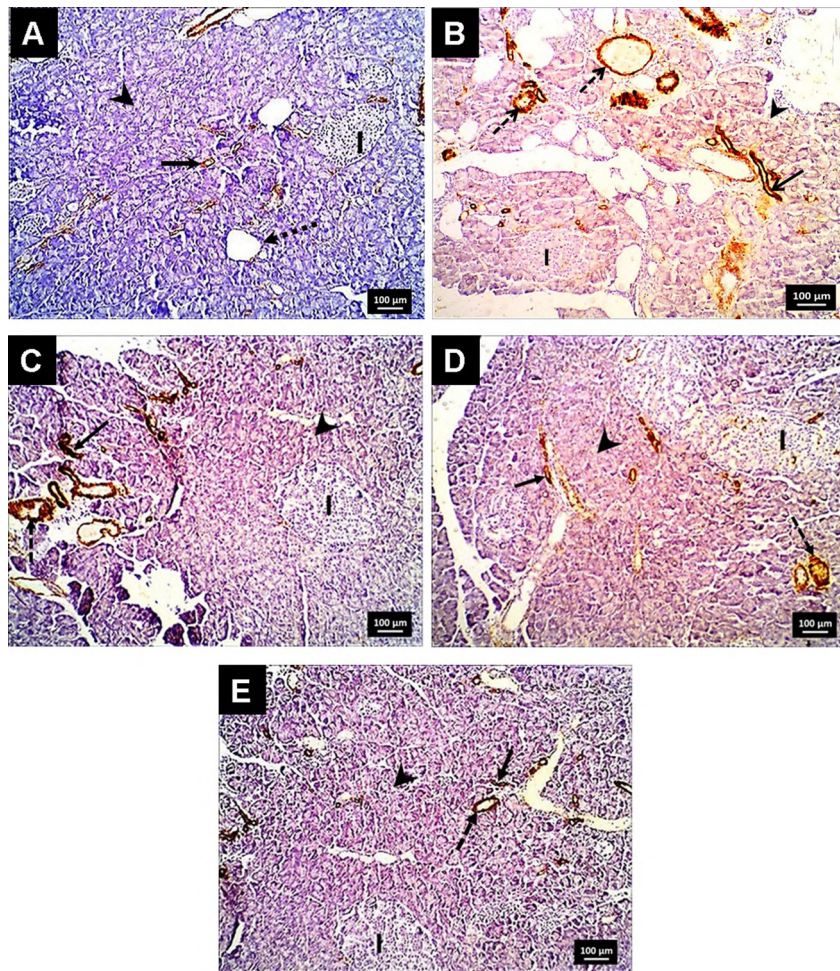


Fig. 4.- α -SMA-immunostained sections of the pancreas. **(A)** Control group; showing minimal brownish immunoreactivity around the blood vessels and negative expression in the wall of the and islet of Langerhans. **(B)** CP group showing intense brownish immunoreactivity in the stroma, around the blood vessels and ducts with minimal expression in the islet of Langerhans. **(C)** CP+BMSCs group showed moderate brownish immunoreactivity in the stroma, around the blood vessels, ducts, and negative expression in the islet of Langerhans. **(D)** CP+Taurine group showed moderate brownish immunoreactivity in the stroma, around the blood vessels and ducts, and minimal expression in the islet of Langerhans. **(E)** CP+BMSCs+Taurine group showed minimal brownish immunoreactivity in the stroma, around the blood vessels and ducts, and negative expression in the islet of Langerhans. α -SMA immunostaining, x100; scale bars = 100 μ m. A-SMA, α smooth muscle actin; CP, chronic pancreatitis; BMSCs, bone marrow mesenchymal stem cells.

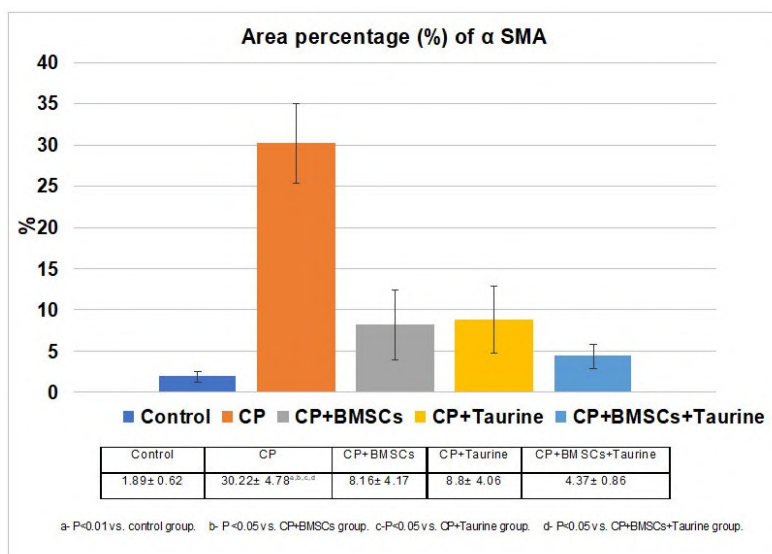


Fig. 5.- Area percentage of α -SMA among different study groups (Mean±SD).

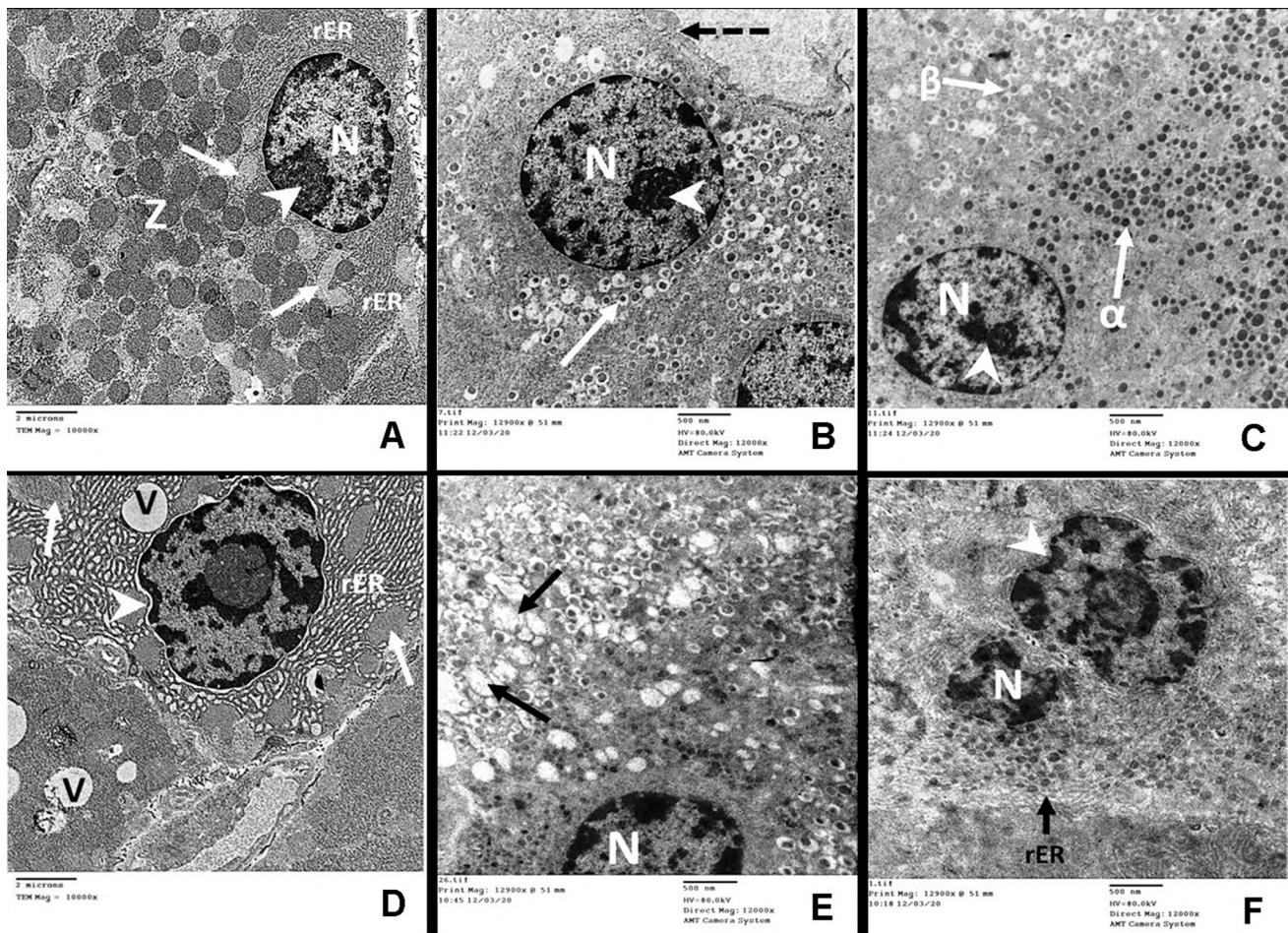


Fig. 6.- Electron micrograph sections of the pancreas. **(A)** A pancreatic acinar cell of the control group showing euchromatic nucleus (N) and nucleolus (arrowhead), apical electron-dense zymogen granules (Z), rough endoplasmic reticulum (rER), and mitochondria (arrows) (TEM, $\times 10,000$). **(B)** β cell of the islets of Langerhans of the control group showing a euchromatic nucleus (N) with prominent nucleolus (arrowhead) and secretory granules with variable electron-dense cores and wide halos (arrow), the endothelium of the blood capillary (dashed arrow) (TEM, $\times 12,000$). **(C)** α cell of islets of Langerhans of the control group showing euchromatic nuclei (N) with prominent double nucleoli (arrowhead) and variable size electron-dense secretory granules (α arrow), β cell appear adjacent to α cell with β cell granules (β arrow) (TEM, $\times 12,000$). **(D)** A pancreatic acinar cell of the CP group showing dilation and focal degranulation of the rough endoplasmic reticulum (rER), mitochondrial swelling (arrows), irregular nuclear membrane (arrowhead), and vacuolation of the cytoplasm (V) (TEM, $\times 10,000$). **(E)** β cell of islets of Langerhans of the CP group showing euchromatic nuclei (N) and some empty secretory granules (arrows) (TEM, $\times 12,000$). **(F)** α cell of islets of Langerhans of the CP group showing shrinkage of the nucleus with increased heterochromatin (N), irregular nuclear membrane (arrowhead), dilated cisternae of the rough endoplasmic reticulum (rER arrow), and minimal secretory granules. (TEM, $\times 12,000$). Scale bars: A, D = 2 μm ; B, C, E, F = 500 nm. TEM, transmission electron microscope; CP, chronic pancreatitis.

membrane and the granule proper. The endoplasmic reticulum of the rough type was seen filling the cytoplasm (Fig. 6B). The α cell of the islets of Langerhans had euchromatic nuclei with prominent nucleolus and variable size electron-dense secretory granules (Fig. 6C). The CP group showed massive acinar cell necrosis with minimal zymogen granules, dilation and focal degranulation of the rough endoplasmic reticulum, mitochondrial swelling with vacuolation of the cytoplasm, and some contained electron-dense bodies. The blood capillaries were congested with increased collagen deposition around their walls (Fig. 6D). The

atrophied islet of Langerhans was noticed as a small hypodense area with irregular nuclei. β cell of islets of Langerhans showed some empty secretory granules (Fig. 6E). While the α cells showed wide, rough endoplasmic reticulum and irregular shrunken nucleus (Fig. 6F), the ultrastructure of the CP+BMSCs group showed marked improvement. However, some zymogen granules were still less electron-dense than that of the control group, and some mitochondrial edema was still present (Fig. 7A). The β and α cells of the islets of Langerhans showed a structure resembling that of the control group (Fig. 7B and C) respectively. The

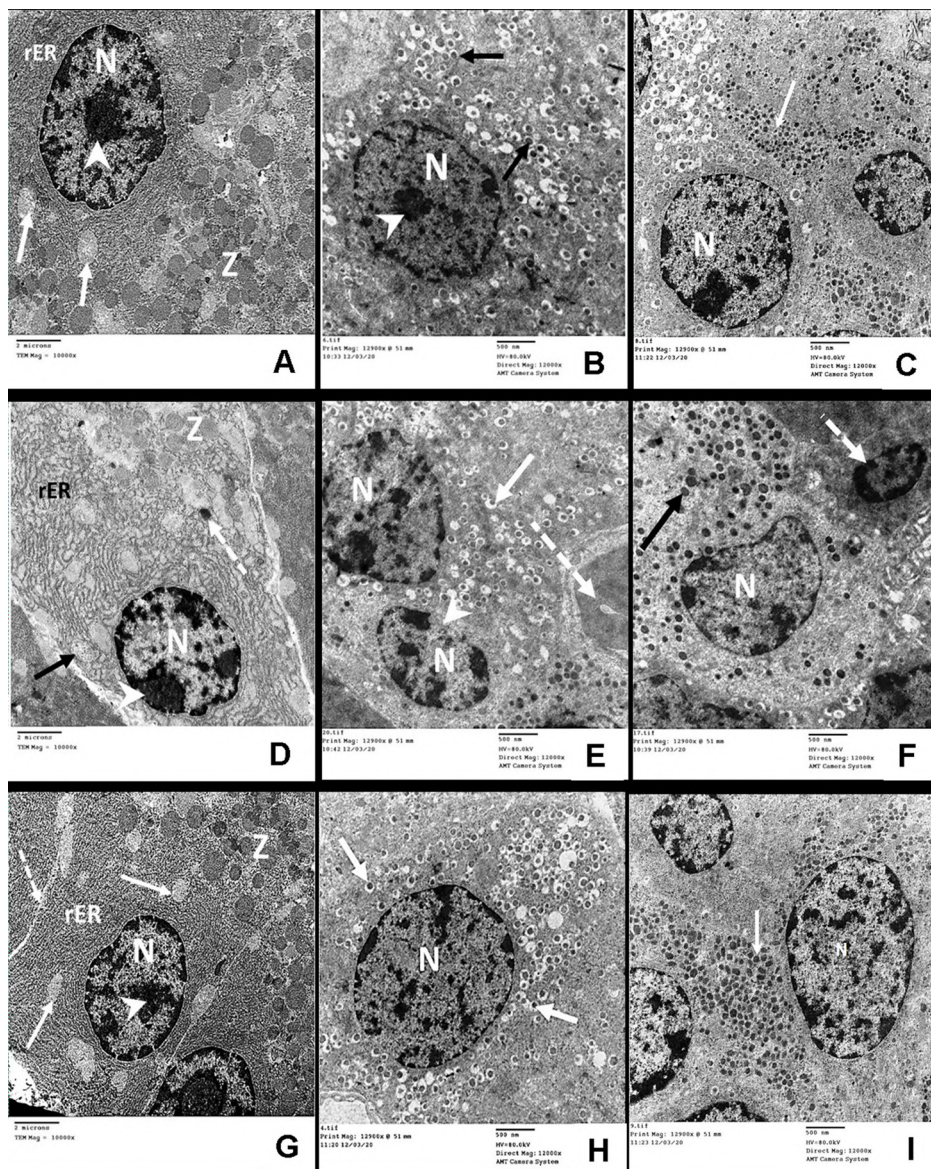


Fig. 7.- Electron micrograph sections of the pancreas. **(A)** The acinar cell of the CP+BMSCs group showing euchromatic vesicular nucleus (N), nucleolus (arrowhead), rough endoplasmic reticulum (rER), hypodense zymogen granules (Z) and some mitochondrial edema (arrows) (TEM, x10,000). **(B)** β cell of islets of Langerhans of the CP + BMSCs group showing euchromatic nucleus (N) with prominent nucleolus (arrowhead) and variable secretory granules (arrows) (TEM, x12,000). **(C)** α cell of islets of Langerhans of the CP+BMSCs group showing with euchromatic nuclei (N) minimal variable size electron-dense secretory granules (arrow) (TEM, x12,000). **(D)** The acinar cell of the CP+Taurine group showed euchromatic nucleus (N), nucleolus (arrowhead), dilated rough endoplasmic reticulum (rER) with few zymogen granules (Z), swollen mitochondria (arrow), and single electron-dense free ribosome (dashed arrow) (TEM, x10,000). **(E)** β cell of islets of Langerhans of the CP+Taurine group showing euchromatic nucleus (N), and another one with damaged nuclear membrane (arrowhead) secretory granules (arrow) and blood capillary (dashed arrow) (TEM, x12,000). **(F)** α cell of islets of Langerhans of the CP+Taurine group showing euchromatic nucleus (N), another nucleus with chromatin condensation (dashed arrow), and electron-dense secretory granules (arrow) (TEM, x12,000). **(G)** The acinar cell of the CP+BMSCs+Taurine group showed a euchromatic nucleus (N) with prominent nucleolus (arrowhead), mitochondria (arrows), rough endoplasmic reticulum (rER), multiple electron-dense zymogen granules (Z), and intercellular space (dashed arrow) (TEM, x10,000). **(H)** β cell of islets of Langerhans of the CP+BMSCs+Taurine group showing euchromatic nuclei (N), secretory granules (arrows) (TEM, x12,000). **(I)** α cell of islets of Langerhans of the CP+BMSCs+Taurine group showing euchromatic nuclei (N), electron-dense secretory granules (arrow) (TEM, x12,000). Scale bars: A, D, G = 2 μ m; B, C, E, F, H, I = 500 nm. TEM, transmission electron microscope; CP, chronic pancreatitis; BMSCs, bone marrow mesenchymal stem cells.

blood capillaries were seen scattered among the islet's cells with flat endothelium and blood cells in their lumen. The CP group treated with taurine showed moderate restoration of most of the normal cellular architecture with narrow intercellular spaces. Dilatation of the rough endoplasmic

reticulum was still present. The mitochondriae were swollen with the loss of their cisternae. Single free ribosomes appeared as electron-dense dots in the cytoplasm were seen (Fig. 7D). The β cells showed a damaged nuclear membrane (Fig. 7E), while the α cells of the islets of Langerhans

showed a structure resembling that of the control group, but the nucleus had appeared with condensed chromatin (Fig. 7F). The CP+BMSCs+Taurine treated group showed restoration of the architecture of the acinar cell to normal, appearing with a basal euchromatic nucleus and prominent nucleolus, while their apical part showed multiple zymogen granules. Abundant parallel stacks of rough endoplasmic reticulum speckled with ribosomes were noticed, with scattered mitochondria containing parallel shelf-like cisternae (Fig. 7G). The β cells of the islets of Langerhans showed euchromatic nuclei with prominent nucleoli, abundant secretory granules of varying sizes with an electron-lucent halo structure between the limiting membrane and surrounding the granule proper (Fig. 7H). The α cells of the islets of Langerhans had euchromatic nuclei with prominent nucleolus and variable size electron-dense secretory granules (Fig. 7I).

DISCUSSION

MSCs are considered an excellent candidate for cell therapy due to their low immunogenicity, accessibility, broad differentiation potential, and immunomodulatory effects (Lennon and Caplan, 2006). Additionally, it was demonstrated that antioxidant supplementation led to a significant reduction in the oxidative stress related to pancreatic fibrosis in CP (Swentek et al., 2021).

In the current study, the subcultured BMSCs had a well-defined polygonal appearance with many cytoplasmic processes. This is consistent with Yusop et al. (2018), who noticed that MSCs have a heterogeneous morphology. Moreover, BMSCs showed moderate positive expression of the CD 44 marker and negative expression for CD 34, which agrees with He et al. (2018). Therefore, the BMSCs used in this study met the standard criteria of the ISCT, which include adherence to the culture flask and positive expression of stromal CD markers (Dominici et al., 2006).

SRY gene could be traced in the pancreas of groups treated with the BMSCs. These findings agree with Zhao et al. (2016), Sun et al. (2017). However, Eggenhofer et al. (2012) reported that MSCs were found only in the lung for 1 hour after

intravenous infusion and in the liver for 24 hours after infusion, and could not be tracked in any other organ 72 hours after infusion.

In the current study, there was a significant reduction in the body weight of rats of groups CP, CP+ MSCs, and CP+Taurine when compared to the control group. This is in accordance with Robles et al. (2014) and Sharma et al. (2017), who reported a significant decrease in the body weight of rats with L-arginine-induced CP. In controversy, Obafemi et al. (2018) demonstrated that rats were losing weight at the beginning of the experiment but started to regain weight two weeks after induction of the tissue injury.

Reduced body weight of L-arginine-treated rats could be due to increased peroxidation of lipids as a consequence of L-arginine-induced oxidative stress, as explained by Sharma et al. (2017). Additionally, it was reported that the degree of weight loss corresponded directly to the degree of malnutrition. This malnutrition was the result of malabsorption and maldigestion of fats with increased metabolic activity due to the inflammatory components of CP (Rasmussen et al., 2013).

On the other hand, rats in the CP+BMSCs+Taurine treated group showed a significant increase in body weight when compared to the CP group. This is in agreement with Mas et al. (2006), who reported that taurine-treated group could gain weight after 28 days of taurine treatment.

Regarding the weight of the pancreas, the present study showed a significant decrease in the CP group. This is in agreement with Sharma et al. (2017) and Obafemi et al. (2018). There was a significant increase in the pancreatic weight of CP groups treated with MSCs alone or in combination with taurine respectively. This is in the match with Sun et al. (2017) who noticed an increase in pancreatic weight after MSCs treatment.

In the present study, the CP group had severely destructed pancreatic architecture histologically and ultra-structurally. This is consistent with Zhang et al. (2016), Kanika et al. (2015) and Sharma et al. (2017), who used L-arginine for the induction of chronic pancreatitis. On the other hand, the current findings are contradictory to Obafemi et al. (2018) who noticed self-recovery of

pancreatic injury after four weeks of induction of CP.

It was reported that L-arginine increases oxidative and nitrosative stress, as it is metabolized to NO; a highly reactive free radical; by NO synthase leading to inflammatory response and finally acinar cell damage (Buchwalow et al., 2013). This is associated with the infiltration of monocytes and macrophages into the injured pancreas which releases TNF- α , which is one of the main factors for CP-induced inflammatory response, as TNF- α can increase the release of other pro-inflammatory factors (such as IL-6). It also increases the expression of chemokines and adhesion molecules, which induces the recruitment of inflammatory cells (Chen et al., 2019). Furthermore, massive enlargement and damage of the pancreatic mitochondria were attributed to the appearance of intracytoplasmic vacuolation, as mentioned by Kui et al. (2014).

The hydropic degeneration of the islets of Langerhans of the CP group was in agreement with Roy et al. (2020), who noticed the depletion of β cells with the development of diabetes mellitus in CP rats. On the other hand, Robles et al. (2014) and Sharma et al. (2017) reported that no morphological changes were affecting the islets of Langerhans. The survival of the islet cells is due to the protective effects of regenerating proteins produced by acinar cells of the pancreas, which are upregulated at the early stage of CP and then reduced as a result of the exocrine pancreatic insufficiency late in CP (Huan et al., 2019).

In the present work, the interlobular duct showed glandular hyperplasia. In accordance, human exocrine tissues from patients with pancreatitis showed ductal metaplasia and cell proliferation (Zhou and Melton, 2018).

BMSCs made some improvements to pancreatic tissue architecture, which are compatible with Zhou et al. (2013) and Sun et al. (2017). On the other hand, Kawakubo et al. (2016) reported that MSCs transplantation could not suppress tissue fibrosis and inflammatory cell infiltration. It was reported that the paracrine secretion of growth factors by MSCs has antiapoptotic, immunoregulatory, and angiogenic functions, which reduce

the number of neutrophils and mast cells binding to vascular endothelial cells and limit the mobilization of these cells to the area of damage (Andrzejewska et al., 2019).

Treatment with taurine showed restoration of most of the normal pancreatic architecture. This is consistent with Mas et al. (2006), Shirahige et al. (2008) and Matsushita et al. (2012). Taurine improves the tissue oxidative stress and inhibits TNF, which enhances the survival of acinar cells and prevents complications of pancreatitis (Mas et al., 2006). Also, taurine increases the cellular content of the BCL-2 protein which has antiapoptotic properties (Matsushita et al., 2012).

Combined treatment with BMSCs and taurine showed restoration of the normal pancreatic architecture. Antioxidant treatment behaves like a preconditioning agent that increases the secretion of favorable MSCs paracrine activity and decreases the risk of the early death of the engrafted MSCs in the damaged tissue (Lou et al., 2019). Moreover, Mashyakhly et al. (2021) demonstrated that taurine increased the TERT gene expression, which encodes the TERT protein, which is responsible for the restoration of telomeric length in MSCs.

In the present study, results revealed that the CP group had an intense expression of α -SMA. This is in accordance with Qin et al. (2014), Zhou et al. (2013) and Sun et al. (2017). Normally, PSCs are inactive and characterized by α -SMA-negative staining. In CP, inflammatory cells release many inflammatory mediators, which activate the PSCs that start to change their morphological features and increase the expression of α -SMA, and then start to secrete extracellular matrix components, such as collagen and fibronectin leading to pancreatic fibrosis (Qin et al., 2014). In the current study, rats of the CP+Taurine group presented with less pancreatic fibrosis. This is compatible with Shirahige et al. (2008).

In the present work, rats of the CP+ BMSCs and CP+ BMSCs+Taurine groups showed a decrease in the expression of α -SMA when compared to the CP group. This agrees with Qin et al. (2014) and Zhou et al. (2013), who reported that MSCs could suppress PSCs activity by inhibiting the infiltration of

inflammatory cells, and the expression of fibrosis-related inflammatory cytokines and chemokines. On the other hand, Kawakubo et al. (2016) showed that the MSCs did not affect pancreatic fibrosis.

Also in the present work, it was found that the group treated with both BMSCs and taurine showed minimal expression of α -SMA around the stromal blood vessels. This agrees with Liao et al. (2020), who reported that the antioxidant could promote MSCs viability through reducing the oxidative stress and inhibit cell apoptosis.

CONCLUSION

In the current study, L-arginine injection resulted in severe pancreatic tissue destruction and fibrosis observed in CP. On the other hand, treatment with BMSCs or taurine alone could improve the pancreatic histopathological changes to some extent, but the combination of both BMSCs or taurine in the CP+ BMSCs+Taurine treated group resulted in good results regarding the pancreatic histopathological changes, pointing to an antioxidant's synergistic effect on both.

REFERENCES

- AN J, BEAUCHEMIN N, ALBANESE J, ABNEY T, SULLIVAN A (1997) Use of a rat cDNA probe specific for the Y chromosome to detect male derived cells. *J Androl*, 18: 289-293.
- ANDRZEJEWSKA A, LUKOMSKA B, JANOWSKI M (2019) Concise review: mesenchymal stem cells: from roots to boost. *Stem Cells*, 37(7): 855-864.
- BOZZOLA JJ, RUSSELL LD (1999) Specimen preparation for scanning electron microscopy. In: Bozzola JJ, Russell LD (eds). *Electron microscopy: principles and techniques for biologists*. 2nd edition (Ch. 3). Jones and Bartlett.
- BUCHWALOW I, SCHNEKENBURGER J, TIEMANN K, SAMOILOVA V, BANKFALVI A, POREMBA C, SCHLEICHER C, NEUMANN J, BOECKER W (2013) L-arginine-NO-cGMP signaling pathway in pancreatitis. *Sci Rep*, 3: 1899.
- CHEN L, CHEN Y, YUN H, JIANLI Z (2019) Tetramethylpyrazine (TMP) protects rats against acute pancreatitis through NF- κ B pathway. *Bioengineered*, 10(1): 172-181.
- DOMINICI M, LE BLANC K, MUELLER I, SLAPER-CORTENBACH I, MARINI F, KRAUSE D, DEANS R, KEATING A, PROCKOP D, HORWITZ E (2006) Minimal criteria for defining multipotent mesenchymal stromal cells. The International Society for Cellular Therapy position statement. *Cytotherapy*, 8(4): 315-317.
- EGGENHOFER E, BENSELER V, KROEMER A, POPP F, GEISSLER E, SCHLITT H, BAAN C, DAHLKE M, HOOGDUIJN M (2012). Mesenchymal stem cells are short-lived and do not migrate beyond the lungs after intravenous infusion. *Front Immunol*, 3: 297.
- GONZÁLEZ AM, GARCIA T, SAMPER E, RICKMANN M, VAQUERO EC, MOLERO X (2011) Assessment of the protective effects of oral tocotrienols in arginine chronic-like pancreatitis. *Am J Physiol Gastrointest Liver Physiol*, 301(5): G846-855.
- HE Q, YE Z, ZHOU Y, TAN WS (2018) Comparative study of mesenchymal stem cells from rat bone marrow and adipose tissue. *Turk J Bio*, 42: 477-489.
- HUAN C, STANEK A, MUELLER C, OU P, DONG S, ZHANG J, ABDEL-NABY R, GRUESSNER R (2019) Loss of Reg proteins' protection of islet β cells in chronic pancreatitis: A potential mechanism for the pathogenesis of type 3c diabetes. *Curr Opin Endocr Metab Res*, 5: 21-28.
- HUANG S, XU L, SUN Y, WU T, WANG K, LI G (2015) An improved protocol for isolation and culture of mesenchymal stem cells from mouse bone marrow. *J Orthop Translat*, 3(1): 26-33.
- JC C, PARKS RW (2021) Chronic pancreatitis-update on pathophysiology and therapeutic approaches. *Indian J Surg*, 83(Suppl 3): 701-708.
- KANIKA G, KHAN S, JENA G (2015) Sodium butyrate ameliorates L-arginine-induced pancreatitis and associated fibrosis in wistar rat: role of inflammation and nitrosative stress. *J Biochem Mol Toxicol*, 29(8): 349-359.
- KAWAKUBO K, OHNISHI S, FUJITA H, KUWATANI M, ONISHI R, MASAMUNE A, TAKEDA H, SAKAMOTO N (2016) Effect of fetal membrane-derived mesenchymal stem cell transplantation in rats with acute and chronic pancreatitis. *Pancreas*, 45(5): 707-713.
- KUI B, BALLA Z, VEGH E, PALLAGI P, VENGLOVECZ V, IVÁNYI B, TAKÁCS T, HEGYI P, RAKONCZAY Z (2014) Recent advances in the investigation of pancreatic inflammation induced by large doses of basic amino acids in rodents. *Lab Invest*, 94(2): 138-149.
- LENNON DP, CAPLAN AI (2006) Isolation of rat marrow-derived mesenchymal stem cells. *Exp Hematol*, 34(11): 1606-1607.
- LI X, BAI J, JI X, LI R, XUAN Y, WANG Y (2014) Comprehensive characterization of four different populations of human mesenchymal stem cells as regards their immune properties, proliferation and differentiation. *Int J Mol Med*, 34(3): 695-704.
- LIAO N, SHI Y, WANG Y, LIAO F, ZHAO B, ZHENG Y, ZENG Y, LIU X, LIU J (2020) Antioxidant preconditioning improves therapeutic outcomes of adipose tissue-derived mesenchymal stem cells through enhancing intrahepatic engraftment efficiency in a mouse liver fibrosis model. *Stem Cell Res Ther*, 11(1): 237.
- LOTIFYA A, SALAMA M, ZAHRAN F, ELENA J, AHMED B, SOBH M (2014) Characterization of mesenchymal stem cells derived from rat bone marrow and adipose tissue: a comparative study. *Int J Stem Cells*, 7(2): 135-142.
- LOU D, YE J, YANG L, WU Z, ZHENG W, ZHANG H (2019) Icarin stimulates differentiation of bone marrow-derived mesenchymal stem cells (BM-MSCs) through activation of cAMP/PKA/CREB. *Braz J Pharm Sci*, 55: 95-104.
- MARRACHE F, PENDYALA S, BHAGAT G, BETZ KS, SONG Z, WANG TC (2008) Role of bone marrow-derived cells in experimental chronic pancreatitis. *Gut*, 57(8): 1113-1120.
- MAS MR, ISIK AT, YAMANEL L, INAL V, TASCI I, DEVECİ S, MAS N, COMERT B, AKAY C (2006) Antioxidant treatment with taurine ameliorates chronic pancreatitis in an experimental rat model. *Pancreas*, 33(1): 77-81.
- MASHYAKHY M, ALKAHTANI A, ABUMELHA A, SHARROUFNA RJ, ALKAHTANY MF, JAMAL M, ROBAIAN A, BINALRIMAL S, CHOCHAN H, PATIL VR, RAJ AT, BHANDI S, REDA R, TESTARELLI L, PATIL S (2021) Taurine augments telomerase activity and promotes chondrogenesis in dental pulp stem cells. *J Pers Med*, 11(6): 491.
- MATSUSHITA K, MIZUSHIMA T, SHIRAHIGE A, TANIOKA H, SAWA K, OCHI K, TANIMOTO M, KOIDE N (2012) Effect of taurine on acinar cell apoptosis and pancreatic fibrosis in dibutyltin dichloride-induced chronic pancreatitis. *Acta Med Okayama*, 66(4): 329-334.
- OBAFEMI TF, YU P, LI J, DAVIS JM, LIU K, CHENG B, ZHAO X, SHEN Q, YOUNES M, KO TC, CAO Y (2018) Comparable responses in male

and female mice to cerulein-induced chronic pancreatic injury and recovery. *JOP*, 19(5): 236-243.

QIN T, LIU CJ, ZHANG HW, PAN YF, TANG Q, LIU JK, WANG YZ, HU MX, XUE F (2014) Effect of the $\kappa\text{B}\alpha$ mutant gene delivery to mesenchymal stem cells on rat chronic pancreatitis. *Genet Mol Res*, 13(1): 371-385.

RASMUSSEN HH, IRTUN Ø, OLESEN SS, DREWES AM, HOLST M (2013) Nutrition in chronic pancreatitis. *World J Gastroenterol*, 19(42): 7267-7275.

ROBLES L, VAZIRI ND, LI S, MASUDA Y, TAKASU C, TAKASU M, VO K, FARZANEH SH, STAMOS MJ, ICHII H (2014) Dimethyl fumarate protects pancreatic islet cells and non-endocrine tissue in L-arginine-induced chronic pancreatitis. *PLoS One*, 9(9): e107111.

ROY A, SAHOO J, KAMALANATHAN S, NAIK D, MOHAN P, POTTAKKAT B (2020) Islet cell dysfunction in patients with chronic pancreatitis. *World J Diabetes*, 11(7): 280-292.

SCUTERI A, MONFRINI M (2018) Mesenchymal stem cells as new therapeutic approach for diabetes and pancreatic disorders. *Int J Mol Sci*, 19(9): 2783-2796.

SHARMA S, RANA SV, RANA S, BHASIN DK, NADA R, MALHOTRA S (2017) Severe chronic pancreatitis due to recurrent acute injury: non-invasive chronic pancreatitis model of rat. *JOP*, 18(2): 107-120.

SHIRAHIGE A, MIZUSHIMA T, MATSUSHITA K, SAWA K, OCHI K, ICHIMURA M, TANIOKA H, SHINJI T, KOIDE N, TANIMOTO M (2008) Oral administration of taurine improves experimental pancreatic fibrosis. *J Gastroenterol Hepatol*, 23(2): 321-327.

SINGH VK, YADAV D, GARG PK (2019) Diagnosis and management of chronic pancreatitis: a review. *JAMA*, 322(24): 2422-2434.

SOLIMAN ME, KEFAFY MA, MANSOUR MA, ALI AF, ESA WA (2014) Histological study on the possible protective effect of pentoxifylline on pancreatic acini of L-arginine-induced acute pancreatitis in adult male albino rats. *Menoufia Med J*, 27(4): 801-808.

SUN Z, GOU W, KIM D, DONG X, STRANGE C, TAN Y, ADAMS DB, WANG H (2017) Adipose stem cell therapy mitigates chronic pancreatitis via differentiation into acinar-like cells in mice. *Mol Ther*, 25(11): 2490-2501.

SWENTEK L, CHUNG D, ICHII H (2021) Antioxidant therapy in pancreatitis. *Antioxidants (Basel)*, 10(5): 657.

WHITCOMB DC, FRULLONI L, GARG P, GREER JB, SCHNEIDER A, YADAV D, SHIMOSEGAWA T (2016) Chronic pancreatitis: an international draft consensus proposal for a new mechanistic definition. *Pancreatology*, 16(2): 218-224.

YANG L, SHEN J, HE S, HU G, SHEN J, WANG F, XU L, DAI W, XIONG J, NI J, GUO C, WAN R, WANG X (2012) L-cysteine administration attenuates pancreatic fibrosis induced by TNBS in rats by inhibiting the activation of pancreatic stellate cell. *PLoS One*, 7(2): e31807.

YUSOP N, BATTERSBY P, ALRAIES A, SLOAN AJ, MOSELEY R, WADDINGTON RJ (2018). Isolation and characterisation of mesenchymal stem cells from rat bone marrow and the endosteal niche: a comparative study. *Stem Cells Int*, 2018: 6869128.

ZHANG W, ZHAO J, PING F, LIU Z, GU J, LU X (2016) Effect of dimethyl fumarate on rats with chronic pancreatitis. *Asian Pac J Trop Med*, 9(3): 261-264.

ZHAO H, HE Z, HUANG D, GAO J, GONG Y, WU H, XU A, MENG X, LI Z (2016) Infusion of bone marrow mesenchymal stem cells attenuates experimental severe acute pancreatitis in rats. *Stem Cells Int*, 2016: 7174319.

ZHOU C, LI M, QIN A, LV S, ZHU X, LI L, DONG Y, HU C, HU D, WANG S (2013) Reduction of fibrosis in dibutyltin dichloride-induced chronic pancreatitis using rat umbilical mesenchymal stem cells from Wharton's jelly. *Pancreas*, 42(8): 1291-1302.

ZHOU Q, MELTON DA (2018) Pancreas regeneration. *Nature*, 557(7705): 351-358.